**INTERNATIONAL JOURNAL OF OPTIMIZATION IN CIVIL ENGINEERING**
***Int. J. Optim. Civil Eng., 2022; 12(4):517-543***

# A MODIFIED GENETIC ALGORITHM STRATEGY FOR OPTIMAL SENSOR\ EXCITER PLACEMENT CAPABLE OF TIME DOMAIN STRUCTURAL IDENTIFICATION

S. H. Mahdavi[*, †1] and K. Azimbeik[2]
[1]*Department of Civil Engineering, Higher Education Complex of Bam, Bam, Iran*
[2]*Department of Civil Engineering, Sharif University of Technology, Tehran, Iran*

## ABSTRACT

This paper presents an efficient wavelet-based genetic algorithm strategy for optimal sensor\exciter placement (OSP\OEP) in large-scaled structures suitable for time-domain structural identification. For this purpose, a wavelet-based scheme is introduced in order to improve the fitness evaluation of GA-based individuals capable of using adaptive wavelets. A search domain reduction (SDR) strategy is proposed to reduce the wide space of initial unknowns corresponding to enormous degrees-of-freedom in large systems. The proposed reduction strategy is carried out at three stages according to the use of different wavelet functions. Furthermore, a multi-species decimal GA coding system is modified for a competent search around the local optima. In this regards, a local operation of mutation is presented in addition with regeneration and reintroduction operators. It is deduced that, the reliable OSP\OEP strategy prior to the time-domain identification will be achieved by those procedures dealing with minimizing the distance of simulated responses for the entire system and condensed system considering the excitation effects. The numerical assessment on the appropriateness and capability of the proposed approach demonstrates the substantially high computational performance and fast convergence of the proposed OSP\OEP strategy, especially in large-scaled structural systems. It is concluded that, the robustness of the proposed OSP\OEP procedure lies on the precise and fast fitness evaluation at larger sampling rates which resulting in the optimum evaluation of the GA-based exploration and exploitation phases towards the global optimum solution.

**Keywords**: optimal sensor placement; optimal exciter placement; time-domain identification; wavelet analysis; genetic algorithm.

Received: 30 March 2022; Accepted: 20 July 2022

[*]Corresponding author: Department of Civil Engineering, Higher Education Complex of Bam, Bam, Iran
[†]E-mail address: sh.mahdavi@bam.ac.ir (S. H. Mahdavi)

## 1. INTRODUCTION

Over the past two decades, structural identification and damage detection have been the area of great technical and scientific interests [1-6]. Generally, structural identification procedures fall into two main categories. The first category involves time-domain strategies considering the actual time-history of structural responses [7]. Whereas, the second is frequency-domain methods dealing with the modal parameters and natural frequencies of structural systems [8-12]. For many reasons the first category of structural identification is more beneficial than the second category [7]. For instance, the frequency-domain methods are based on the modal parameters (linear super position), thus they are limited for only linear systems. Another drawback in performing frequency-domain approaches is that, the information for higher structural modes are not reliable. In contrast, time-domain methods do not require to measure frequencies and modal parameters, and instead they directly utilize time-history information including all structural modelled modes.

Generally, sensor\exciter (actuator) placement and optimization are of great significance in variety of vibration control problems. The effect of sensor and actuator configurations in large and flexible structural systems has been investigated by many researchers for active and passive control of structures [13-19]. In addition, Roh and Park [20] presented that, there are two main issues considering the structural identification and control of large systems. One is how to select those of exciters to perform a frequency-domain identification and the other is how to choose actuator locations to control the large system. Their proposed methods of optimal sensor\exciter placement were based on quantitative measures of modal degree of controllability and excitability. Furthermore, genetic algorithms (GAs) have been extensively employed for optimal sensor and actuator placement in diverse structural control problems [18,21-24].

There are many attempts have been delivered for optimal sensor placement (OSP) in frequency-domain. An enhanced GA strategy was presented for OSP of structural health monitoring systems by considering the performance function based on damage detection [23]. A decimal GA strategy was proposed by Liu et al. [24] for OSP in large scaled spatial lattice structures. The fitness evaluation was based on modal strain energy and modal assurance criterion suitable for frequency-domain structural identification. Their proposed method was using an operation of forced mutation to alter the identical possibilities obtained from a set of strings (namely, an individual). However, the proposed forced mutation was randomly operated and the major drawback of classical GA was still remained (in referring to the disability of GA for an efficient search around the local optima towards the global solution). The idea of forced mutation was introduced and it was deduced that the convergence rate speed is faster than penalty-based operations [24]. Moreover, theoretical and computational difficulties arising from the OSP configuration for prediction of structural uncertainties were addressed by Papadimitriou [25]. In addition, the influence of parametric uncertainties was investigated on OSP in a truss bridge by Castro et al. [26]. Mahdavi and Razak (2016) proposed a modified GA-based strategy for optimal sensor placement capable of time-domain structural identification. They demonstrated that for such aim, the improved operations of genetic coding provide the superiority of their proposed strategy in dealing with OSP problems. It was shown that the application of enhanced discrete GA coding will result in promising outputs for reliable time-domain identification problems [27]. The

review of relevant literature shows that frequency-domain methodologies were comparatively employed for OSP and the influence of exciter position was not thoroughly addressed in contributing with time-domain system identification problems.

A framework was proposed for OSP in flexible structures with multi-dimensional mode shapes. The strength of signals was evaluated by effective independence and modified variance methods. The number of sensors was determined using a threshold for modal assurance criterion between predicted ones from observations and target mode shapes. It was shown that, a Krigings model could be determined as the sum of linear regression and random errors as the indicator of stochastic process. Furthermore, the effect of Krigings parameters was investigated in order to get the minimum number of sensors [28]. Li et al. [29] highlighted the main shortcoming of conventional sensor placement schemes for frequency-domain identification methods where these approaches do not take into account the actual structural responses and loading conditions (including exciter placement). They improved a novel load dependent method for OSP considering the structural modal features, exciter location as well as loading conditions. They concluded that, in order to gain an acceptable identification, not only the optimal sensor location but also the exciter positions have to be accounted. Ostachowicz et al. presented a comprehensive review of OSP in dealing with structural health monitoring problems [30]. Moreover, the sensor placement solutions are optimized using a parallel optimization framework based on the competent genetic algorithm, leading to a number of features that enrich the application flexibility [31]. In order to minimize the effects of noise on the damage detection process, efficient methods for OSP based on a new geometrical viewpoint for damage detection in structures was presented by Beygzadeh et al. (2013) [32]. An efficient data-driven method to obtain the optimal sensor subset from the entire candidate sensor set was proposed in Ref. [33]. In order to make the model more robust to outliers and overcome the limitation of inconsistent coefficients for multiple class optimization problem, the proposed method introduces a special norm to realize the similar sparse structures of coefficients. A hybrid optimization algorithm including finite element grids updating for optimal sensor placement was proposed based on effective independence method and sensor distribution index, in order to improve the algorithm efficient and reduce the redundancy information simultaneously [34]. Furthermore, a structural damage detection-oriented multi-type sensor placement method with multi-objective optimization was developed by Lin et al. (2018) [35].

Based on the literature review presented here, one may conclude that, an efficient layout of sensor configuration and exciter locations are crucial to optimally measure structural responses. In other words, an accurate measurement for a trustworthy time-domain structural identification strategy cannot be achieved, regardless of the exciter locations. As a consequence, OSP\OEP strategies play the underlying role in achieving the reliable identification results. Therefore, the improvement of available methods for OSP\OEP capable of time-domain structural identification is unavoidable.

On the other hand, wavelet analysis has attracted tremendous attentions of scientists and engineers in different disciplines of science and technology. Fundamentally, multi-resolution analysis and localization properties are the main strength points of this powerful tool for solving the variety of partial and ordinary differential equations [36]. In addition, the dynamic analysis of single-degree-of-freedom (SDOF), multi-degrees-of-freedom (MDOF) and framed structures were improved by using a wavelet-based method capable of using

only the simple Haar and the first kind of Chebyshev wavelets (FCW) [36]. An extension of the wavelet-based scheme for structural simulation of large-scaled space structures has also been developed by the same researchers using complex Chebyshev and Legendre wavelets [37]. A comprehensive study was conducted for the analysis of stability and accuracy of results. It was inferred that, the method lies on an unconditionally stable scheme with sufficient accuracy. As an unconditionally stable method, there was no requirement on selecting computational time intervals. Consequently, wide-frequency components of the applied load were accurately approximated by free-scaled operators of wavelet on adaptive collocation points. The property of compatibility provided the possibility of using more collocations regarding to the higher scales. Therefore, broad frequency features were accurately integrated in the vicinity of highly varying structural responses. The achieved results were promising enough so as to implement the proposed method for solving optimization problems. An efficient discrete and modified genetic algorithm was implement based on wavelet analysis for time-domain impact localization in large-scaled structures [38]. It is shown that, among the verity of evolutionary optimization algorithms available for such applications, the employment of multispecies discrete coding provides the superiority of the proposed scheme in addressing the major shortcoming of genetic algorithm.

In this paper, an efficient OSP\OEP strategy is developed by using wavelet-based genetic algorithms suitable for time-domain identification of large-scaled structures. Due to inherent ability of wavelet functions the GA-based fitness evaluation is significantly improved towards the most optimum approach in Section 2. The proposed strategy for OSP\OEP is developed in Section 3. For this purpose, the proposed decimal GA coding system, adopted GA-based operations, the efficient forced mutation for local search, the proposed search domain reduction strategy and fitness evaluation of GA individuals are presented in this section. In addition, Section 4 is devoted to the step-by-step algorithm of the strategy applicable for OSP\OEP in large-scaled structures. Subsequently in Section 5, a brief description is presented for the employed strategy of time-domain structural identification for evaluation purpose. Finally, in order to confirm the validity of results of current study, two numerical applications are discussed in Section 6. The verification study involves OSP\OEP in a simple multi-degrees-of-freedom (MDOF) system and a 3-dimensional (3D) and large-scaled space truss structure.

## 2. OPTIMAL STRUCTURAL SIMULATION USING WAVELETS

Fundamentally, the core of proposed genetic algorithm strategy in this study lies on the optimal structural simulation. The optimum structural simulation using adaptive wavelet functions is thoroughly discussed in Refs. [36,37]. Accordingly, the main characteristics of Haar wavelets, the first kind of Chebyshev wavelets (FCW) and the Legendre wavelets (LW) are presented in these references for implementing in forward dynamic analysis. The underlying idea is to simplify the governing dynamic equilibrium using wavelet operational matrices. For the sake of completeness, a brief description is provided in Appendix B regarding to the computation of wavelet operational matrices of FCW, the second kind of Chebyshev wavelet (SCW) and LW. In addition, it is shown that a signal can be decomposed by scaled and delayed wavelet functions from $t_i$ to $t_{i+1}$ (known as global time)

by dividing time interval to some partitions related to the order of the wavelet. The method of subdividing time domain of a signal into the multiple segments suitable for time-scaled-frequency analysis is known as Segmentation Method (SM). Obviously, if a global time interval is divided into many local subdivisions (namely, collocation points), a set of adaptive segmentations will collectively and intricately cover the signal. Thus, the employed operation on the compatible collocation points can be adaptive with the features of the signal, i.e., frequency content of the signal [36,37]. In this study, $2M$ is taken 4 and refers to the number of partitions in each global time interval with respect to the scale of the proposed wavelet function. For instance, $2M = 2^{j+1}$ represents the $2^{j}$ th scale of LW, SCW or Haar wavelet. Consequently, broad frequency components of either the externally applied load or inherent features of dynamic system are accurately and optimally approximated by free-scaled operators of wavelet on compatible collocation points even for longer time intervals. The emphasis of compatibility lies on the possibility of using more collocations, denoting higher scales, and therefore precisely capturing wide-band frequency features. Eventually, after solving diverse structural dynamic problems, it is concluded that, different scales of SCW simulate the most accurate results. However, LW also achieves satisfactorily reliable results, and the superiority of LW lies on the better computational performance compared with SCW, in referring to the simple computation of operational matrices of LW (Appendix B). In addition, it is deduced that, despite the most optimum cost of analysis by using free-scaled Haar wavelet functions, the accuracy of results using this basis function is not satisfactory.

In addition, the improved Guyan dynamic condensation (IGDC) technique is utilized to reduce the size of structural characteristic's matrices (i.e., stiffness, mass and damping) from the entire structure to the condensed system. For this aim, measured and loading degrees-of-freedom (DOFs) corresponding to the location of exciter obtained from GA-based individuals are selected as master DOFs. Subsequently, the wavelet-based approach is implemented to optimally simulate the structural responses on master DOFs and then feeding the fitness evaluation code. It should be kept in mind that, the use of Gauss-Jordan elimination method in approaching IGDC is essential to avoid computational difficulties and calculating inverse matrices numerous times.

## 3. PROPOSED WAVELET BASED GA STRATEGY FOR OSP\OEP

Until now, GAs have proved to be a robust and competence tool for especially combinatorial optimization problems such as OSP\OEP. As the OSP\OEP problems proceed with searching on the population of alternative design variables rather than a single point in the design domain, the use of GA has a demonstrated merit over traditional optimization strategies. The first underlying step to employ GA is to adopt the most appropriate coding system. One of the superior features of the proposed wavelet-based GA algorithm herein is employing a search domain reduction (SDR) scheme at three stages of optimization. Subsequently, the proposed wavelet-based GA strategy, coding system and its operations are presented in this section.

*3.1 GA coding system and operations*

In this study, the decimal coding system is proposed for representing the design variables of OSP\OEP problem. The structure of the proposed GA population is shown in Fig. 1. As it is shown in this figure, each population is divided into 4 sub-populations (namely, species).

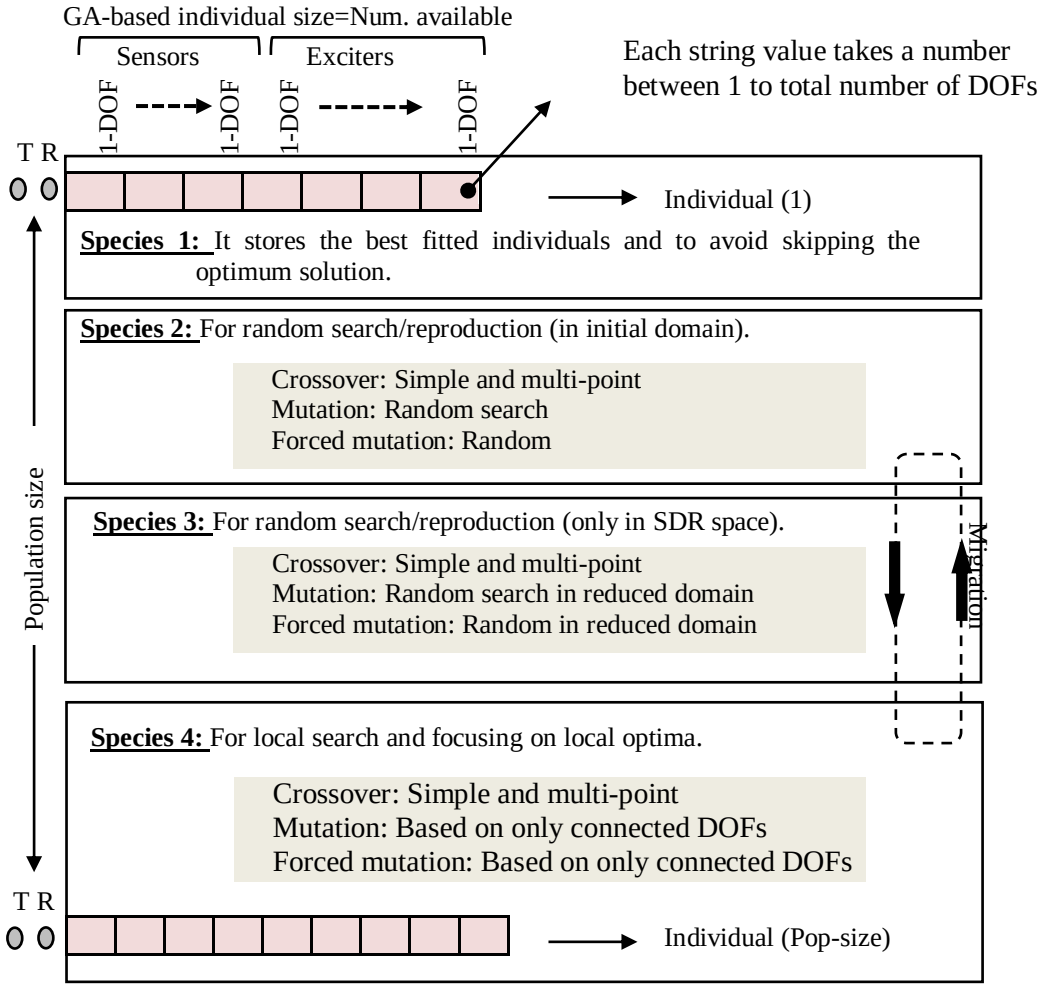


Figure 1. The construction of the proposed multi-species DGA strategy for OSP\OEP

One of the significant modification of the proposed strategy is adopting different species in each population to overcome the issue of local optima. In fact, one of the major issue with using simple GA is that the possible solutions may converge to the local optima and cannot escape towards the global optima. As it is shown in Fig. 1, species 1 stores the best fitted individuals (chromosomes) and it is adopted to avoid skipping the optimum solution. The size of each individual is $n$ (the number of available sensors and exciters to be used).

Each string may take a decimal number from one to the total number of DOFs. In this study, in order to improve the computational competency of OSP\OEP strategy for large-scaled structures (in referring to the enormous number of DOFs) a search domain reduction

(SDR) approach is implemented. For this purpose, the feasible search domain governing the unknown sensor\exciter locations is reduced at three steps (except for species 2) corresponding to the use of different wavelet operators for fitness evaluation (Fig. 3). The proposed SDR strategy is regulated based on selecting the only connected DOFs and relatively all adjacent DOFs to the connected members of the best solution results from the former generations (adjacent DOFs are not essentially connected to the obtained positions for sensors\exciters). In addition, species 2 is constructed for random search on possible locations (DOFs) in original search domain (all DOFs existing in the structure) for adding sensor\exciter. It guaranties the comprehensive search in the entire search space so that the global solution is not skipped. However, for an efficient analysis, the size of this species may be chosen far lesser than other species. Furthermore, species 3 is adopted for searching on the entire reduced domain including both, all connected DOFs and adjacent ones. While, species 4 is organized for focusing on the local optima (only connected DOFs to the fitted solutions). The regeneration is carried out only on species 2 and 3, involving the complete replacement of this species to random possible solutions in original search domain and reduced domain corresponding to the species 2 and 3, respectively. This allows species 2 and 3 to efficiently search on the search domain for possible solutions, while species 4 refines previously generated solutions. It is observed that, the small number of regeneration is needed, however, it can be defined by the user (3 regenerations are operated in this study). Eventually, for the purpose of an efficient search on good solutions in species 4 (around local optima), reintroduction is necessary. In this way, at a prescribed number of times individuals in spices 1 (best solutions) are inserted into spices 4. It is found that the large number of this operation usually provides better convergence and therefore better results. However, for selecting the number of reintroduction it should be taken into account that, the best solutions from species 1 are supposed to be improved in species 4 and it will be accomplished after several generations. The reproduction process is carrying out by well-known crossover and natural mutation operations. Two types of simple and multi point crossover are operated on selected pair individuals in species 2, 3 and 4 based on the prescribed crossover rate. In performing the crossover or natural mutation operations, the same location may be placed with two sensors\exciters in an individual, synchronously. In order to change the identical sensor\exciter locations in an individual, the operator of forced mutation is executed.

This operator changes the string value randomly in original search domain and reduced domain until an unrepeated possible sensor\exciter location for species 2 and 3, respectively. The distinct advantage of the proposed forced mutation in this study is that, it searches only on connected DOFs (as sensor\exciter locations) for strings placed in the fourth species. This allows an efficient search around the local optima. Furthermore, the ratio of the natural mutation operation can be reduced in order to achieve a reasonable compatibility of GA-based operations. Finally, in order to exchange information between species 2, 3 and 4, the migration is operated to transfer information from these species. This operation involves swapping randomly selected chromosomes between these two species. The migration rate controls the number of times to operate this operation.

Moreover, one issue for storing the best optimum solutions in species 1 is that a same individual can be selected several times for this species. This will result in saturating spices 1 and therefore an excessive focus will be on one possible solution (or sub-optimal

solutions) rather than focusing on many good possible solutions. To overcome this problem, the tagging procedure is introduced. First, all individuals are assigned as 0 tag and if an individual is moved into species 1 its tag will be changed to 1. This tag accompanies individual wherever it moves. Once this individual is altered by any GA-based operations (representing new possibilities), the tag is changed back to 0 and it could be selected again in the first species. To clarify the coding system and the proposed GA-based operations for OSP\OEP, a simple population corresponding to a 3D truss is illustrated in Fig 2. It should be noted that the main contribution of this study involves using decimal GA coding, however, in Fig. 2(c) a binary coding representation is also provided. It will be shown later that, the binary coding for particularly OSP\OEP in large-scaled structures is neither practical nor possible due to the high dissipative storage space for saving the optimum solutions of numerous DOFs. In contrast, decimal GA coding enlarges the individual's storage and leads the satisfactorily fast convergence of the proposed algorithm.

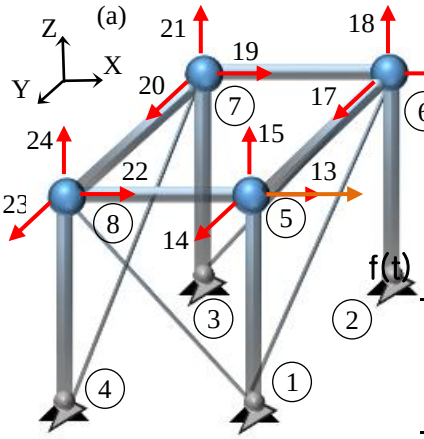


- The considered pin-jointed truss with 12 transitional DOFs (13-24).
- The first 12 DOFs are fixed due to the supports.
- Tagging is initially set to 0 for all Ind.
- Ranking is initially set to 1 for all Ind.

(b)

| Variables | 2 Sens. 1 Exc. 13-24 | 13-24 | 13-24 | T | R |
|---|---|---|---|---|---|
| Species 1 | 16 | 21 | 18 | 1 | 1 |
| Species 2 | 20 | 17 | 22 | 0 | 1 |
| Species 3 | 19 | 23 | 24 | 0 | 1 |
| Species 4 | 16 | 20 | 18 | 0 | 1 |

(c)

| Var.(Av. DOFs) | 2 Sens. 1 Exc. 13-24 | | | | | 13-24 | | | | | 13-24 | | | | | T | R |
|---|---|---|---|---|---|---|---|---|---|---|---|---|---|---|---|---|---|
| Species 1 | 1 | 0 | 0 | 0 | 0 | 1 | 0 | 1 | 0 | 1 | 1 | 0 | 0 | 1 | 0 | 1 | 1 |
| Species 2 | 1 | 0 | 1 | 0 | 0 | 1 | 0 | 0 | 0 | 1 | 1 | 0 | 1 | 1 | 0 | 0 | 1 |
| Species 3 | 1 | 0 | 0 | 1 | 1 | 1 | 0 | 1 | 1 | 1 | 1 | 1 | 0 | 0 | 0 | 0 | 1 |
| Species 4 | 1 | 0 | 0 | 0 | 0 | 1 | 0 | 1 | 0 | 0 | 1 | 0 | 0 | 1 | 0 | 0 | 1 |

(d)

| Var.(Av. DOFs) | | 2 Sens. 1 Exc. 13-24 | 13-24 | 13-24 | T | R |
|---|---|---|---|---|---|---|
| Individual pair before crossover | Parent 1 | 16 | 21 | 18 | 0 | 1 |
| | Parent 2 | 13 | 16 | 24 | 0 | 1 |
| Developed individual pair after crossover | Offspring 1 | 13 | 21 | 24 | 0 | 1 |
| | Offspring 2 | 16 | 16 | 18 | 0 | 1 |
| Developed individual pair after forced mutation | Offspring 1 | 13 | 21 | 24 | 0 | 1 |
| | Modified Offspring 2 | 16 | 18 | 18 | 0 | 1 |

Figure 2. The proposed GA-based strategies for OSP\OEP, (a) a 3D truss example with 12 DOFs, 2 available (Av.) sensors (Sens.) and 1 exciter (Exc.), (b) decimal GA coding (DGA), (c) binary GA coding (BGA), (d) the operation process of forced mutation

The pin-jointed truss system shown in Fig. 2(a) consists of 8 nodes, 12 transitional DOFs, and therefore 12 possible locations (DOFs 13-24) for sensors\exciters. For simplification purpose, it is assumed that 2 number of sensors and 1 exciter are available with only 1 individual (Ind) per species (4 spices). This constructs the population size of (4×Ind) × (available sensors + exciters = 3) as shown in Fig. 2(b). Using the decimal representation of strings placed in species 2, Fig. 2(b), means that possible locations for the sensors and exciters are on the $20^{th}$ and $17^{th}$ DOFs and $22^{nd}$ DOF, respectively. The binary representation of the considered population size is displayed in Fig. 2(c). As it is shown in Fig. 2(d), after paring selected individuals for reproduction (namely, parents) the two-points crossover is operated and resulting in the developed individuals (namely, offspring 1 and 2). It can be seen that, developed offspring 2 contains one identical DOF ($16^{th}$) for sensor location. Obviously, one of these strings should be changed to the new possible solution due to the fact that, practically it is meaningless to define the same placement for two sensors. In this regards, forced mutation operator is designed to change one of the same values to another value which is not existed in this individual. For instance, in this example one of the value of 16 can be changed to a connected DOF e.g., 18. It should be noted here that, the new value 18 could be selected randomly from the entire search domain of 13-24 (as long as it is not repeated in the same individual). In contrast, if it is located in species 4 (which is designed for local search) the priority of selection is with the connected DOFs. This provides a comprehensive search around the best results obtained from previous generations. It can be seen in Fig. 2(d) that, an identical location $18^{th}$ may be selected for sensor and exciter placement in a single individual. However, it will be shown later that, such placement is not optimum solution due to the condensation of structural characteristic's matrices for one lesser master DOF which leads the lower fitness value for this individual.

*3.2 Fitness evaluation and selection*

As it was mentioned earlier, the main robustness of the proposed GA herein lies on the optimal structural simulation using adaptive wavelets. In other words, by improving the GA-based fitness evaluations (FE) using adaptive wavelets, not only the convergence of results is accelerated but also the computational efficiency of the proposed OSP\OEP strategy is significantly improved. Accordingly, the fitness of each individual in all species proposed in this study are evaluated by adding the inverse of total sum of squared errors between the simulated time-history of accelerations for the entire structure (Acc1) and reduced structure (Acc2) based on the master and omitted DOFs developed in GA-based strings as follows:

$$\text{Fitness} = \frac{1}{\varepsilon + \frac{\sum(\text{Acc1} - \text{Acc2})^2}{\text{DOF}_{\text{Master}}}} \tag{1}$$

In Eq. (1), $\text{DOF}_{\text{Master}}$ represents all master DOFs including measured DOFs for sensor placement and DOFs with applied force (the location of exciters). $\varepsilon$ may take a small value of 0.001 to prevent computational difficulties. Later, the selection procedure is carried out by allocating the probability of selection to each individual due to its final fitness. Fundamentally, the high performance of any GA strategy is the resultant of the quality of FE. For this reason,

in order to magnify the differences between different fitness values, a ranking procedure is employed to obtain the probabilities within each species. In this regards, the fitted individual is ranked the total number of population size and the rest are descended due to the value of the fitness function (it is shown in Figs. 1 and 2). The notable point is using adaptive wavelets for FE at small sampling rates. This significantly improves the fitness values and thus rapidly yields the convergence rate. The layout of the proposed wavelet-based FE is illustrated in Fig. 3.

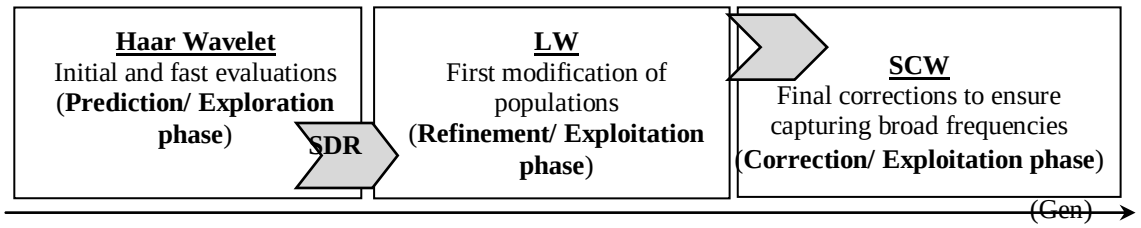


Figure 3. Implementation of adaptive wavelets for OSP\OEP through the proposed DGA_W strategy

As it is shown in Fig. 3, the proposed strategy involves a very fast prediction of variables by using simple and 2D Haar wavelets on optimum collocations. This phase may be interpreted as the exploration phase and there are most relevant variations around the local optima. Afterwards, the initial search domain which in fact lies on a broad space of the possible DOFs (as the sensor\exciter locations) is reduced (for species 3 and 4) based on the connected and adjacent DOFs to the best fitted results located at the first row of the population size. At the second stage of the strategy, the probability of selecting different OSP\OEP have been refined by using three dimensional LW for fitness evaluation of individuals as the same sampling rate as was considered for the first step. Accordingly, this stage is adopted for the exploitation phase where small variations around the global optima existed. In addition, the last SDR is implemented on species 3 and 4. Finally, employing the accurate SCW for fitness evaluation guarantees the promising solutions being selected at the last stage of the strategy. In this way, all details of input/output signals are collectively captured on adaptive collocation points, and therefore the last corrections on the OSP\OEP are optimally ascertained until the prescribed convergence rate is achieved (namely, the final exploitation phase). The motivation behind the proposed development arises from the fact that the overall computational efficiency of the OSP\OEP strategy for large number of possible scenarios is rigorously dependent on optimally reducing the feasible solutions in search domain for numerous possible solutions towards the most optimal scenarios. It should be kept in mind that, because of utilizing more precise wavelet functions progressively, the SDR is not applied on the second species so as it ensures an efficient random search for global optimum solutions.

## 4. STEP-BY-STEP ALGORITHM FOR OSP\OE

The OSP\OEP is accomplished by adopting the decimal GA strategy (DGA) using adaptive wavelets for FE (it is designated by DGA_W) in addition with conducting an efficient SDR strategy. However, with the same proposed DGA algorithm, the use of Newmark's constant-

average time integration scheme for FE will be investigated later for comparison purpose (it is designated by DGA_N).

The proposed procedure involves reintroduction, regeneration and artificial selection of ranked individuals. To guarantee that species 4 (designed for the local search around the best fitted results) operates on a set of desirable solutions, the reintroduction is essential. The schematic flowchart of the proposed DGA_W is depicted in Fig. 4. With reference to Fig. 3, three runs and relatively two SDR are carried out corresponding to Haar, LW and SCW. It should be emphasized that, in this study $2M$=4 (collocation points) is taken for three wavelet basis functions.

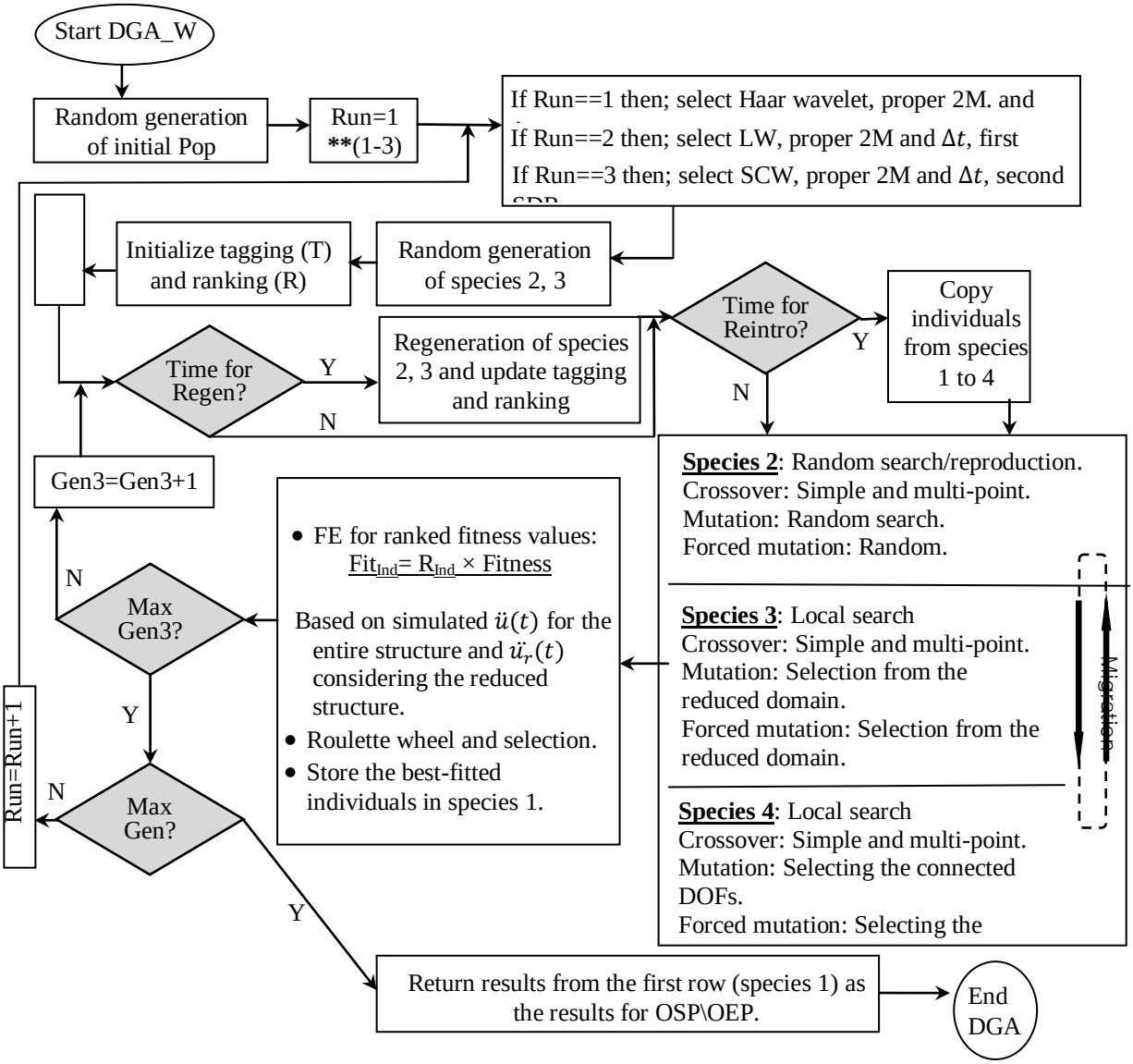


***** Gen = 3 × Gen3.

****** Three runs are considered as regeneration parameter.

Figure 4. The algorithm of proposed DGA_W strategy using adaptive wavelet functions

## 5. TIME-DOMAIN STRUCTURAL IDENTIFICATION USING MODIFIED GAS

In order to verify and validate results obtained from the proposed OSP\OEP algorithm, a water cycle optimization algorithm (WCA) is conducted for time-domain structural identification [38]. The aforementioned strategy lies on minimization of the distance between actual measured accelerations and simulated accelerations obtained for the predicted model. Presuming the same fitness function as in Eq. (1), hence, Acc1 may be referred to the measured accelerations while Acc2 denotes the simulated accelerations. Accordingly, for comparison purpose, a known mass problem is formulated through the identification strategy based on different OSP\OEP scenarios obtained by the proposed algorithm. The overall process of each string (representative of stiffness value for each element) is illustrated in Fig. 5 for stiffness identification of known mass problems in time domain.

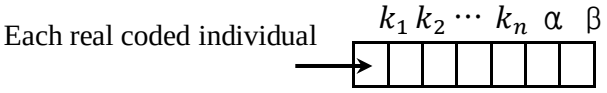


Figure 5. The layout of each individual for the WCA strategy for stiffness identification of known mass problems

Moreover, two procedures are considered for GA-based FE. First, the FE is achieved using Newmark's constant-average acceleration method for simulating the time-history of acceleration (designated by MGA herein) at very small sampling rates (short time intervals should be utilized for capturing the entire details). While the second approach involves the implementation of adaptive wavelets at reasonably larger samplings (designated by WGA) for simulating the accelerations.

## 6. NUMERICAL APPLICATIONS

Actually, the numerical effectiveness of the proposed wavelet-based algorithm for structural dynamic simulation is well evaluated in Refs. [36,37]. In this section, the appropriateness and capability of the proposed DGA strategy for OSP\OEP are numerically examined on two structural systems. For this purpose, two structures are considered, involving a 5 DOFs shear building as well as a 3D and large-scaled truss system. It is to be noted that, the application of binary GA coding (BGA) is impractical for the second example due to the enormous DOFs and so the dissipative storage capacity is much more than the proposed DGA. Furthermore, the identification results corresponding to the obtained scenarios for OSP\OEP are comparatively investigated by using Newmark's constant-acceleration scheme (MGA) and the wavelet-based approach (WGA). In addition, for both cases considered, the mass of structures is lumped at each transitional DOF. Moreover, damping effect is taken into account by adopting the well-known Rayleigh damping by setting the damping ratio of

5% for the first two modes. The related damping constants (α and β) are presumed as unknown values in the identification process. To achieve a comprehensive evaluation, the CPU computational time (as indication of the cost of analysis) is considered for different strategies, which was recorded with a same hardware environment (Intel_R, Xeon_R, CPU E5-1620 V2 @ 3.7 GHz, 64 GB RAM, Operation 64 bit). Fundamentally, the very important step prior to performing the proposed DGA strategy for OSP\OEP is selecting the propitious parameters for GA-based operations. For this aim, some preliminary studies were carried out for each numerical application in order to determine the most reliable GA parameters. The underlying goal of these studies was to identify balanced GA parameters that will give consistently desirable results. It should be taken into consideration that, for different applications, different combinations of GA parameters will have different effects due to the variations across the structural systems and external excitation. Subsequently, the DGA parameters utilized for verification study of OSP\OEP are displayed in Table 1.

Table 1: DGA Parameters utilized for verification study (OSP\OEP)

| | Ex. 1 | Ex. 2 |
|---|---|---|
| Pop-size (species 1-4) | 6+4+20+6 | 30+10+30+30 |
| Generations | 3×10 | 3×150 |
| Crossover rate | 0.8 | 0.6 |
| Natural mutation rate | 0.05 | 0.1 |
| Migration rate | 0.05 | 0.05 |
| Regeneration | 3 | 3 |
| Reintroduction | 6 | 45 |

It is to be pointed out that, the distinguishable advantage and the superiority of the proposed DGA_W strategy fall into two aspects. First, involving the practice of the proposed strategy for OSP\OEP in large-scaled problems, which the performance of GA is considerably enhanced by the proposed SDR operation, multi-species and local search algorithm. Second, the wavelet-based scheme for optimum FE (known as the core of GA) especially for large-scaled systems. Whereby, the high frequency ranges and then large sampling rates (data points) are mostly the focus of interest in order to extract the entire features of dynamic responses. Considering the second point of view, implementing an efficient approach for FE is essential, where the fitness values generally lie on a small value. As a consequence, simple GAs finds it very difficult to be converged and therefore using an improved GA is inevitable.

### *6.1 A five story MDOF shear system*

Fig. 6 illustrates a five-story shear building considered for the first numerical application. Shear building states for the only transitional DOF exciting at each story. The structural characteristics (i.e., the mass and stiffness of each story) as well as the externally applied loading $f(t)$ are shown in the figure. In addition, a schematic view of selecting the master and omitted DOFs is depicted in Fig. 6 corresponding to the different OSP\OEP scenarios. The first 2 sec of vibration is considered for simulating the structural responses at the sampling rate of 500 S/s and 100 S/s corresponding to the use of Newmark (DGA_N) and

wavelet methods (DGA_W), respectively. Furthermore, the noise-free input/output (I/O) data is utilized for this application. In order to clarify the optimization procedure, the first one second time-history of accelerations is depicted in Fig. 7 in referring to the various OSP\OEP scenarios. The first left-hand column corresponds to the OSP scenarios when there is only 1 available sensor, while the next 2 columns implies the OSP for 2 available sensors. In addition, the simulated time-history of accelerations for complete measurement is shown by a plain line in blue, compared with a dashed red line for considered OSP\OEP. As it is illustrated in Fig. 7(a), the goal of the OSP\OEP is to minimize the difference between these two time-history records. For instance, the minimum average error e (%) was computed for OSP\OEP1 as 0.047%, when the exciter's location is at DOF 3. On the contrary, this value declined to about 0.032% for OSP\OEP2.

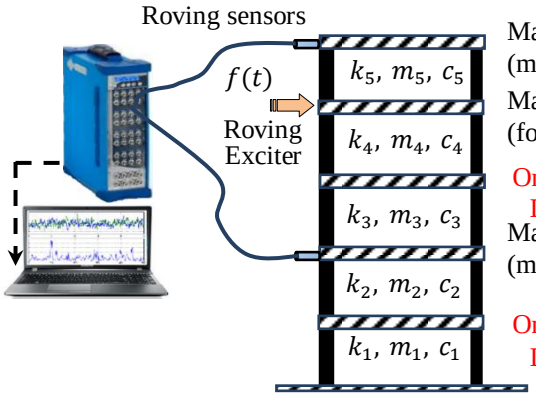


| Story | $k$ (× $10^6$N/m) | $m$ (× $10^3$kg) |
|---|---|---|
| 1 | 400 | 500 |
| 2 | 400 | 400 |
| 3 | 300 | 500 |
| 4 | 200 | 300 |
| 5 | 300 | 500 |

$f(t)$= (10e3)× [$\sin(6\pi t)$ + $\sin(15\pi t)$]

Figure 6. A five DOF shear building considered for the first numerical example ($f(t)$ is in N)

Different OSP\OEP scenarios obtained for different available number of sensors is provided in Fig. 7(b). The DGA parameters are taken from Table 1. Data displayed in Fig. 7(b) demonstrate the necessity of measuring the 5$^{th}$ DOF for all obtained OSP\OEP scenarios. In other words, this DOF may be interpreted as the vital DOF for sensor placement. For a detailed comparison, the mean value of error (%) in identified stiffness of all stories is measured and tabulated in Table 2 for different OSP scenarios considering only 1 available sensor and the exciter's location 3. Fig. 8(b) and Table 2, demonstrates the computational robustness of the proposed OSP\OEP strategy for a reliable time-domain structural identification.

Table 2: Mean error (e %) in stiffness identification results for different scenarios proposed for 1 available sensor and exciter

| | Measured DOFs (master) | Omitted DOFs (Omitted) | Exciter DOF (master) | e % for identified stiffness |
|---|---|---|---|---|
| SP (1 sensor) | 1 | 2 , 4 , 5 | 3 | 6.96 |
| | 2 | 1 , 4 , 5 | 3 | 7.15 |
| | 3 | 1 , 2 , 4 , 5 | 3 | 24.77 |
| | 4 | 1 , 2 , 5 | 3 | 8.82 |
| | 5 | 1 , 2 , 4 | 3 | 6.02 |

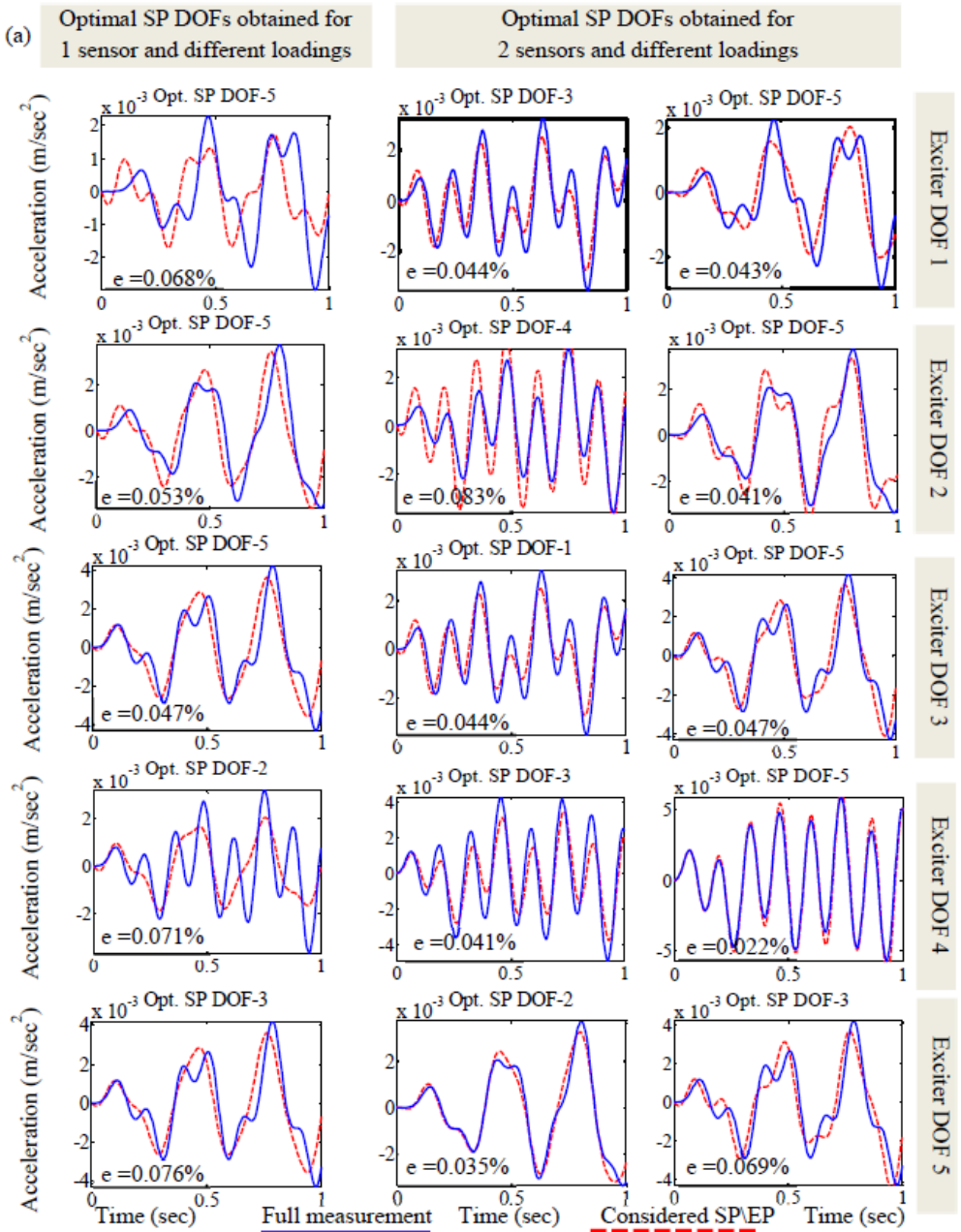


(b)

| 1 Exciter is available for all cases: | OSP | OEP |
|---|---|---|
| OSP\OEP1 DOFs (1 available sensor): | 5 | 3 |
| OSP\OEP2 DOFs (2 available sensors): | 3, 5 | 4 |
| OSP\OEP3 DOFs (3 available sensors): | 1, 3 , 5 | 4 |

Figuer 7. Optimal (Opt.) SP scenarios for 1 and 2 available sensors corresponding to different levels of exciter, (a) comparison of simulated time-history of acceleration for complete and incomplete measurement and obtained Opt. SP, (b) OSP\OEP scenarios

The computational time recorded for OSP\OEP2 using the binary coding GA (BGA_N for using Newark's scheme and BGA_W using the wavelet-based method for FE) and decimal coding (DGA_N and DGA_W) are plotted in Fig. 8(a). As it is shown in this figure, using the wavelet-based approach for FE led the most cost-effective results for both binary and decimal coding systems. However, this figure shows almost a similar performance of BGA and DGA as the considered structure is very small one in scale.

Accordingly, in order to validate the obtained OSP\OEP scenarios, the identification results for implementing WGA and MGA strategies using various placement scenarios are comparatively depicted in Fig. 8(b). In this regards, the first 8 sec of vibration is considered for evaluating the fitness functions. In this figure, OSP\OEP4 indicates the complete measurement for the exciter's location at the 4$^{th}$ level.

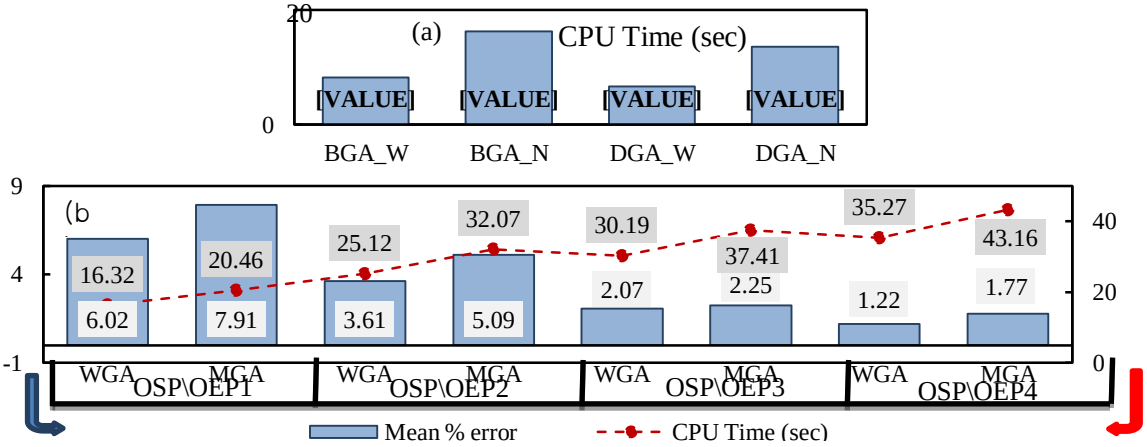


Figure 8. Comparison of results obtained for proposed GA-based algorithms of OSP\OEP and identification, (a) CPU time recorded for OSP\OEP2 using BGA and DGA, (b) CPU time and the mean value of errors in identified stiffness values corresponding to different OSP\OEP

*6.2 A double layered pin-jointed space structure*

Fig. 9 shows the geometry of a double layered pin-jointed and large-scaled truss structure considered for the current numerical application. This structural system comprises 128 truss elements, 41 pinned joints and therefore 111 transitional DOFs. The plain truss structure is hinged at fixed-point supports on four corner joints located at the bottom layer. Moreover, this truss system is constructed with aluminum pipes and the cross-sectional area, mass density and the elastic modulus are provided in Fig. 9(d). The deadweight of structural elements as well as hybrid joints are treated as lumped mass and concentrated at the related nodes. In addition, the first 4 natural frequencies obtained from the finite element model (FEM) are 44.06, 51.9, 63.12 and 74.78 Hz corresponding to the first 4 mode shapes of the structure as shown in Fig. 9(c).

It is very important to keep in mind that, before starting the proposed OSP\OEP strategy or identification approach, the sequence of node numbering should be optimized, initially. Basically, the optimal node numbering of such large-scaled structures plays the underlying role in achieving the highest performance of the optimization approach. In other words, by optimal node numbering of such structures (instead of a random numbering), the bandwidth

of structural characteristics' matrices (i.e., mass, stiffness and damping) is considerably reduced and will result in the reasonably optimum output. In this study, a decimal GA coding is adopted for this purpose and a brief description is provided in Appendix A. Accordingly, the node numbering illustrated in Fig. 9(b) lies on the one of the possible optimal node numbering.

One of the important steps in dealing with the OSP\OEP and structural identification of this structure is to select the appropriate features of the applied excitation through the exciters. The last natural frequency obtained from the FEM lies on 797.33 Hz corresponding to the last mode of vibration. On the other hand, as the proposed strategy requires integration of accelerations, thus it is preferred to utilize a regular and smooth random force for this application rather than a very irregular and complex one. In this regards, a random sinusoidal loading of 40-800 cycle per second (Hz) with the amplitude of [-2, 2] kN generated at 1000 sampling rate, and then it is interpolated to match 200 samplings. Accordingly, the first 1 sec of aforementioned loading is considered for OSP\OEP strategy, while the longer time-history record of 5 sec is selected for identification purpose. The schematic view of the original applied loading and its reduced data length are depicted in Figs. 10(a) and (b) for the first one second of loading, respectively.

As it is apparent in Fig. 10(b), the applied loading (on reduced data length) is smoother than the original one. However, it contains the entire frequency contents in order to extract all characteristics of vibration. Moreover, for FE of DGA_N strategy, a larger sampling rate of 200 S/s is utilized for Newmark's constant-average acceleration method to integrate the entire frequency components. In contrast, in DGA_W strategy the wavelet-based FE of individuals is performed on the reasonably lesser sampling of 100 S/s. The DGA strategies are implemented for determining the OSP\OEP scenarios for different number of available sensors and exciters. The results are displayed in Table 3 for the use of DGA_W and DGA_N. Subsequently, the obtained locations for OSP\OEP1 (availability of 10 sensors and 4 exciters) are also highlighted in Fig. 9(b). Data displayed in Table 3 demonstrates the highest computational efficiency achieved by DGA_W compared to DGA_N. For instance, the CPU time taken known as the indication of the cost of analysis is reduced by about 48% for OSP\OEP1 or by 32% for OSP\OEP3 for the use of DGA_W. In addition, it is observed that the x and y DOFs of node 11 are obtained as the optimal sensor locations for all three OSP considered. As a consequence, locations 11(x,y) may be interpreted as the so-called "vital sensor placements". It is also inferred that, the obtained OEP scenarios for all cases lies on the z direction. This is most probably due to the lesser global rigidity of the structure in this direction in addition with the highest effect of the gravity, which will result in the maximum influence of loading at this direction. More importantly, it is seen that for OSP\OEP3 and above, the z direction of corner nodes is being consistently selected as the optimal sensor locations. The comparison of computational efficiency and convergence rate for OSP\OEP3 displayed in Table 3 using DGA_W and DGA_N are provided in Fig. 11. The emphasis is the fitness value history and CPU time taken in achieving to the prescribed number of generations (3×150 generations).

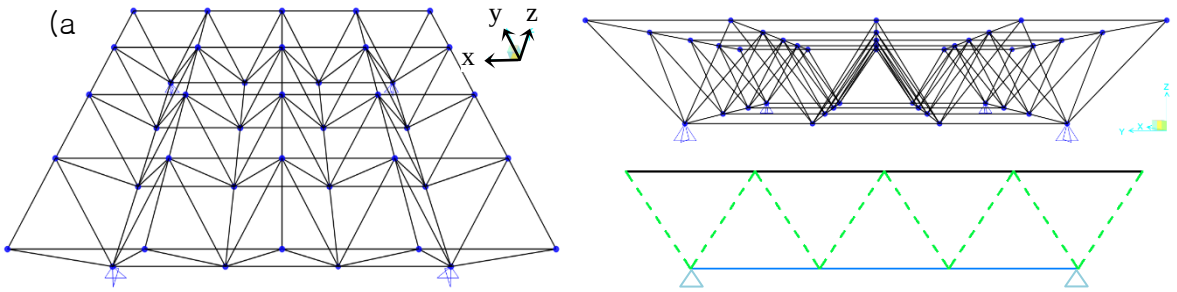


**3D** view; all panels = 2×2 m

**Side** view; height=1 m

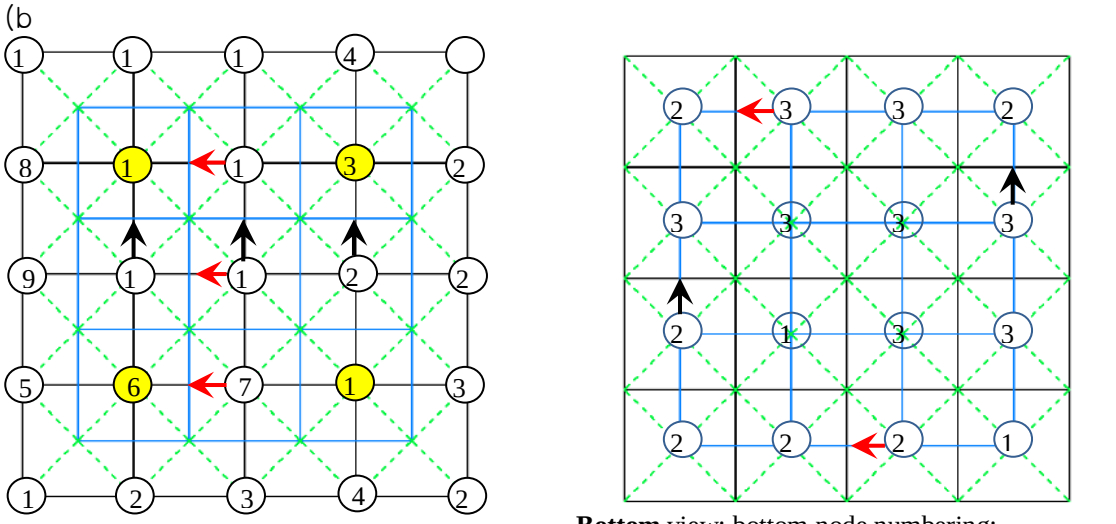


**Top** view; top node numbering; OSP\OEP1

**Bottom** view; bottom node numbering; OSP\OEP1

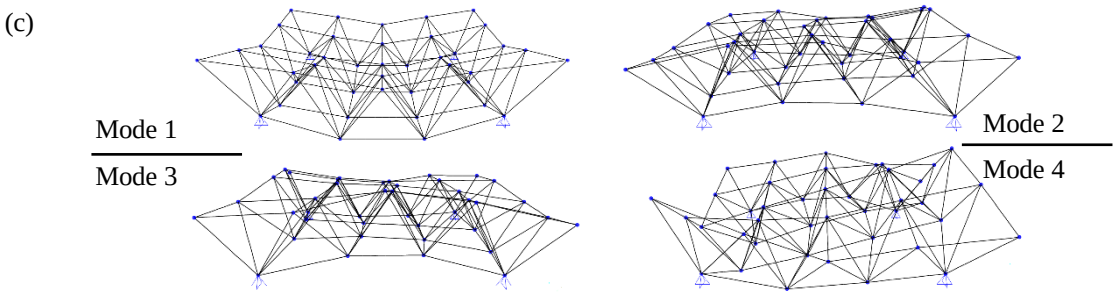


The first four mode shapes

(d)

Cross-sectional area$_{all}$=11.66 cm$^2$, g= 9.81 m/ sec$^2$, E=69 GPa, $\bar{m}$=2600 kg/m$^3$

Figure 9. A double-layered space truss, (a) different views, (b) node numbering and OSP\OEP1 shown in Table 3, (c) the first 4 structural mode shapes, (d) structural characteristics

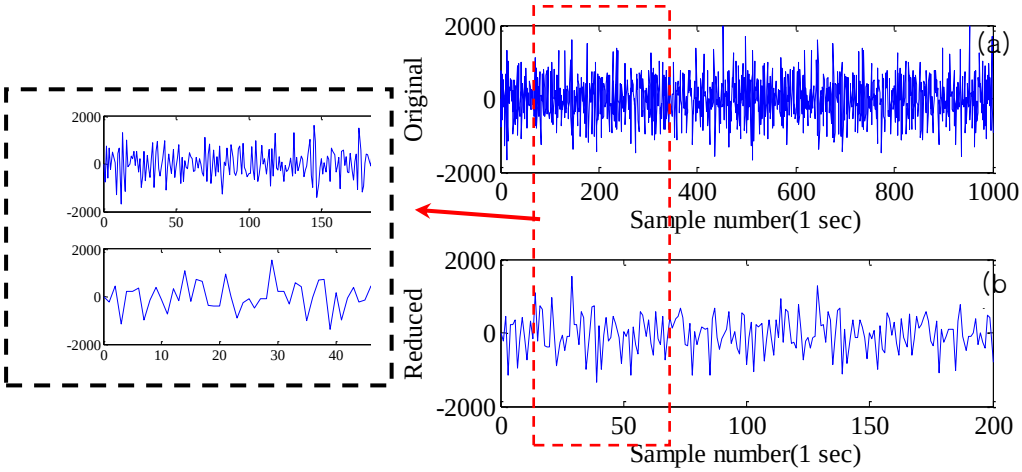


Figure 10. The first one second time-history of input loading, (a) at 1000 sampling, (b) at 500 reduced sampling (reduced data point)

Table 3: OSP\OEP scenarios obtained for different number of available Sens.\Exs. using DGA_W and DGA_N

| | Node number (sensor\exciter in x, y or z directions) | | CPU Time (min) | |
|---|---|---|---|---|
| | | | DGA_W | DGA_N |
| OSP\OEP1(10 Sens., 4 Acts.) | Top: | OSP: 11(x,y), 10(y), 29(y), 7(x), 16(x)<br>OEP: 6(z), 13(z), 15(z), 37(z) | 41.12 | 79.03 |
| | Bottom: | OSP: 27(x), 35(x), 28(y), 39(y) | | |
| OSP\OEP2(20 Sens., 6 Acts.) | Top: | OSP: 3(x), 23(y), 7(x), 15(x), 11(x,y), 29(y), 13(x), 16(x), 10(y), 9(y), 19(x)<br>OEP: 6(z), 13(z), 15(z), 37(z) | 58.32 | 95.44 |
| | Bottom: | OSP: 12(x,y), 31(y), 33(x,y), 27(x), 35(x), 38(y)<br>OEP: 30(z), 32(z) | | |
| OSP\OEP3(30 Sens., 10 Acts.) | Top: | OSP: 3(y), 4(x), 7(x), 23(x), 29(y), 9(x), 10(y), 8(y), 16(x), 19(y), 18(x), 11(x,y), 34(y), 1(z), 14(z), 21(z), 40(z)<br>OEP: 6(z), 13(z), 15(z), 37(z), 7(z), 10(z), 16(z), 29(z) | 70.51 | 103.59 |
| | Bottom: | OSP: 12(x,y), 27(x), 30(y), 31(x,y), 35(x), 36(y), 39(x,y)<br>OEP: 30(z), 32(z) | | |
| OSP\OEP4(10 Acts.) | Complete measurement | | _ | _ |

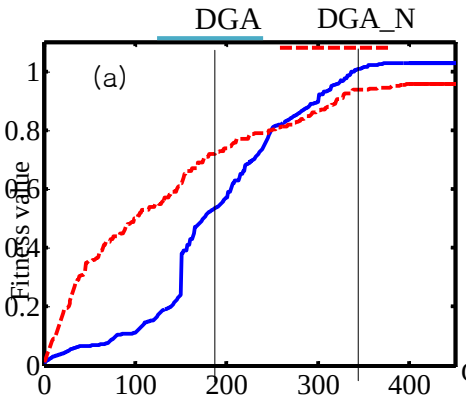


| Simulation scheme and CPU time (min) for 3 stages | | | | |
|---|---|---|---|---|
| | (1) | (2) | (3) | Total |
| DGA_W | Haar | LW | SCW | |
| | 17.22 | 24.51 | 28.78 | 70.51 |
| DGA_N | Newmark | Newmark | Newmark | |
| | 34.53 | 34.53 | 34.53 | 103.59 |

(b)

Figure 11. Comparison of computational efficiency and convergence rate for OSP\OEP3 using DGA_W and DGA_N, (a) fitness value history for 450 generations (Gen), (b) simulation scheme utilized and CPU time taken (min) at 3 stages of SDR

The first notable consideration on the comparison of fitness value histories shown in Fig. 11(a) deals with the highest speed of the convergence due to DGA_W. It is evident from the figure that the GA-based exploration phase (using the fast Haar wavelet before the first SDR) is optimally accomplished by an efficient search around the local optimum solutions. Furthermore, it is seen that the GA-based exploitation phase is broadly focused on the second (using the fast and precise LW operations after the first SDR takes place) and the third stage (using the accurate SCW operations after second SDR), in which that, the small variations around the global optimum solution is existed. In addition, it should be taken into account that the convergence rate and the computational competency are in fact the necessary and sufficient conditions to demonstrate the robustness of the OSP\OEP strategy. The complementary investigation is carried out on the computational efficiency of the proposed strategy in terms of the analysis cost. Accordingly, Fig. 11(b) shows one of the very interesting observations for the use of DGA_W compared to DGA_N in recording the optimum cost of the analysis at three stages that SDR takes place two times corresponding to the employment of different wavelet functions.

Basically, the noise-free input loads are applied through the exciters based on OEP scenarios. However, the inherent of output signals (simulated accelerations) lies on the noise contaminated signals because of the highly varying transient responses due to the complexity of the structure. It can be overtly seen in Fig. 11(a) that the considerably larger fitness value is gained for DGA_W. This is due to the lesser effect of I/O noise to the signal on the proposed DGA_W strategy that has led to the better fitness value.

Eventually, in order to validate the obtained scenarios of OSP\OEP shown in Table 3, the stiffness identification of this structure is conducted 5 times using water cycle optimization algorithm (WCA) on another 4 random OSP\OEP and considered one (as shown in Table 3). The ±15% of axial rigidity (E×Area) of each structural member is treated as unknown stiffness for the sake of comparision.

The first observation from 3×5 times running the identification program as the preliminary tests lies on the best identification results for considered OSP\OEP in Table 3.

This is exactly in agreement with the FE of DGA strategy (implemented for placement) so that the optimization proceeds by minimizing the differences between the time-history of accelerations. Furthermore, it is observed that a very large value of error measurement in identification of one structural element may significantly alter the mean value of error and it could not be as a reliable indication for further comparisons. For this reason, mean value and max value of errors (%) in identified stiffness are presented separately and plotted in Fig. 12 for only OSP\OEPs displayed in Table 3.

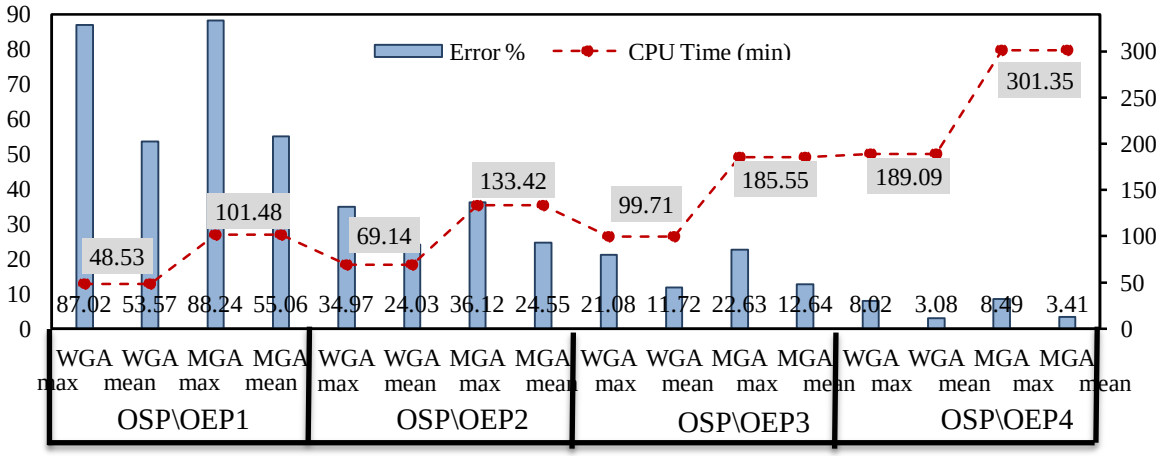


Figure 12. Maximum (max) and mean error (%) in identified stiffness of structural members and recorded CPU time (min) corresponding to different OSP\OEPs shown in Table 3

It was anticipated that, the maximum error values would return to the OSP\OEP1, which about 9% of all DOFs are measured. Consequently, as the number of master DOFs are far lesser than the OSP\OEP4 the most optimum CPU time was recorded for OSP\OEP1 scenario.

## 7. CONCLUSIONS

In this paper, a wavelet-based genetic algorithm strategy is introduced for optimal sensor\exciter placement (OSP\OEP) desirable for time-domain structural identification of large-scaled problems. As the fitness evaluation is benefited by an optimum approach, it is more convenient to perform a multi-species GA for an efficient search on the wide space of feasible solutions (in referring to the numerous DOFs). In this regards, a local operation of mutation is presented through a multi-species decimal coding GA for focusing on the local optima. For this aim, the natural operation of mutation and forced mutation are carried out by selecting the only connected and adjacent DOFs corresponding to different species. It provides a comprehensive search around the local optima while the random search on feasible possibilities proceeds, especially in large-scaled systems. In addition, the fitness evaluation (known as the core of GA) is significantly improved towards the most optimum strategy by using adaptive wavelet functions at three stages. It was inferred that, the

combined multi-species GA may be adopted through the compatible search domain reduction (SDR) suitable for OSP\OEP in large-scaled structures. It was confirmed that, because of the property of unconditional stability of wavelets for structural simulation, from the computational efficiency point of view the fitness evaluation is considerably enhanced by using longer time intervals (shorter sampling rates). The emphasis was on precisely capturing broad frequency contents of the dynamic responses with adaptive collocation points of wavelets. It was concluded that, especially for large-scaled systems with numerous DOFs as possible solutions, by using adaptive wavelets for FE concurrent with an efficient SDR the proposed OSP\OEP strategy is optimally achieved. The far lesser computational time is taken in achieving a prescribed number of generations and resulting in the very cost-effective strategy compared with existing algorithms. It was deduced that, the GA-based exploration and exploitation phases are optimally satisfied by the used of improved fitness evaluation at three stages, and therefore a faster convergence rate is accomplished. In addition, the lesser effects of I/O noise to the signal were recorded for the proposed DGA_W compared with DGA_N. The proposed wavelet-based fitness evaluation has considerably enhanced the computational performance of the OSP\OEP strategy, in terms of reliability, accuracy and computational cost (CPU time). Consequently, for the purpose of a reliable structural identification in time-domain (which is basically based on minimization of the distance between measured and simulated responses), the most accurate OSP\OEP strategy is gained by the proposed strategy with the superior computational performance. Overall, the practice of the proposed strategy in this paper in variety of structural control problems is rigorously recommended.

**Acknowledgements:** The authors wish to acknowledge the financial support from the Higher Education Complex of Bam (Grant No. 81167051400).

## APPENDIX A. OPTIMAL NODE NUMBERING

The brief description on the utilized strategy for optimal node numbering is presented in this section. Basically, a GA-based decimal two-dimensional array coding is proposed for this purpose as tabulated in Table A.1.

Table A.1: Operation process of decimal two-dimensional array strategy for optimal node numbering

| Variables (sequence of nodal numbering for fixed coordinates) | | 1 | 2 | 3 | … | Total number of nodes including supports |
|---|---|---|---|---|---|---|
| Individual gene pair before crossover and forced mutation | Parent 1: | 6 | 19 | 31 | … | 69 |
| | Parent 2: | 2 | 69 | 7 | … | 19 |

The highest fitness of each individual for optimal node numbering returns to the shortest bandwidth of stiffness matrix for structural elements considered, therefore one may obtain fitness=1/(bandwidth[K]).

## APPENDIX B. WAVELET OPERATIONAL MATRICES

This appendix is devoted to the derivation of operation matrix $P$ of integration (corresponding to FCW, SCW and LW). One may approximate the integration of $\Psi(t)$ as (assumption of $k$ =2):

$$\int_0^1 \Psi_{2M}(t)\,dt = P_{2M}\Psi(t) \tag{A.1}$$

As was mentioned before, the subscripts of $\Psi_{2M}$ and $P_{2M}$indicate the dimension of matrices. Correspondingly, the $(2^{k-1}M)\times(2^{k-1}M)$-dimensional operational matrix $P$ for FCW, SCW and LW is derived as [36-39]:

$$P=\frac{1}{2^k}\begin{bmatrix}[L]_{M\times M} & [F]_{M\times M} & F & \dots & F\\ [O]_{M\times M} & [L]_{M\times M} & F & \dots & F\\ O & O & \ddots & \ddots & \vdots\\ \vdots & \vdots & \dots & \ddots & F\\ O & O & \dots & O & L\end{bmatrix} \tag{A.2}$$

where, $M\times M$ square matrices $F$ and $L$ are given as follows:

$$F=\begin{bmatrix}2 & 0 & 0 & \dots & 0 & 0\\ 0 & 0 & 0 & \dots & 0 & 0\\ a_1 & 0 & 0 & \dots & 0 & 0\\ 0 & 0 & 0 & \ddots & \vdots & \vdots\\ \vdots & \vdots & \vdots & \vdots & \ddots & \vdots\\ a_2 & 0 & \dots & \dots & 0 & 0\end{bmatrix},\qquad L=\begin{bmatrix}1 & a_6 & a_9 & a_{12} & \dots & 0 & 0 & 0\\ a_3 & 0 & a_{10} & a_{13} & \dots & 0 & 0 & 0\\ a_4 & a_7 & 0 & a_{14} & \dots & 0 & 0 & 0\\ a_5 & a_8 & a_{11} & 0 & \dots & \vdots & \vdots & \vdots\\ \vdots & \vdots & \vdots & \vdots & \ddots & \vdots & \vdots & \vdots\\ \vdots & \vdots & \vdots & \vdots & \vdots & \ddots & \vdots & \vdots\\ a_{15} & 0 & 0 & \dots & \dots & a_{17} & \ddots & a_{19}\\ a_{16} & 0 & 0 & \dots & \dots & 0 & a_{18} & 0\end{bmatrix} \tag{A.3}$$

There is a similar population for components of $P$ corresponding to considered wavelets. Therefore the coefficients of $a_i$ are obtained as in Table B.1: In order to calculate operation matrix of $P$ for FCW, SCW and LW, a backward algorithm of program coding is recommended. In other words, only the first four rows and columns of $P$ are being calculated, firstly. At the second stage, the components of $P$ being calculated and replaced from the last row and column $M^{\text{th}}$ until computation of the 5$^{\text{th}}$ row and column [36-39].

Table B.1: Coefficients of $\boldsymbol{a_i}$ to calculate operation matrix of integration of FCW, SCW and Legendre wavelets

| $\boldsymbol{a_i}$ | Legendre wavelet | FCW | SCW |
|---|---|---|---|
| $a_1$ | 0 | $-2\sqrt{2}/3$ | $2/3$ |
| $a_2$ | 0 | $\frac{\sqrt{2}}{2}(\frac{1-(-1)^M}{M} - \frac{1-(-1)^{M-2}}{M-2})$ | $\left\|\sin(\frac{M\pi}{2})\right\|\frac{2}{M}$ |
| $a_3$ | $-\sqrt{3}/3$ | $-\sqrt{2}/4$ | $-3/4$ |
| $a_4$ | 0 | $-\sqrt{2}/3$ | $1/3$ |
| $a_5$ | 0 | $\sqrt{2}/4$ | $-1/4$ |
| $a_6$ | $1/\sqrt{3}$ | $1/\sqrt{2}$ | ½ |
| $a_7$ | $-\sqrt{5}/(5\sqrt{3})$ | $-1/2$ | $-1/6$ |
| $a_8$ | 0 | 0 | 0 |
| $a_9$ | 0 | 0 | 0 |
| $a_{10}$ | $\sqrt{3}/(3\sqrt{5})$ | ¼ | ¼ |
| $a_{11}$ | $-\sqrt{7}/(7\sqrt{5})$ | $-1/4$ | $-1/8$ |
| $a_{12}$ | 0 | 0 | 0 |
| $a_{13}$ | 0 | 0 | 0 |
| $a_{14}$ | $\sqrt{5}/(5\sqrt{7})$ | $1/6$ | $1/6$ |
| $a_{15}$ | 0 | $\frac{\sqrt{2}}{2}(\frac{(-1)^{M-3}}{M-3} - \frac{(-1)^{M-1}}{M-1})$ | $(-1)^{M-2}\frac{1}{M-1}$ |
| $a_{16}$ | 0 | $\frac{\sqrt{2}}{2}(\frac{(-1)^{M-2}}{M-2} - \frac{(-1)^{M}}{M})$ | $(-1)^{M-1}\frac{1}{M}$ |
| $a_{17}$ | $-\frac{(2M-3)^{1/2})}{(2M-3)(2M-5)^{1/2}}$ | $\frac{-1}{2(M-3)}$ | $-\frac{1}{2(M-1)}$ |
| $a_{18}$ | $-\frac{(2M-1)^{1/2}}{(2M-1)(2M-3)^{1/2}}$ | $\frac{-1}{2(M-2)}$ | $-\frac{1}{2M}$ |
| $a_{19}$ | $\frac{(2M-3)^{1/2}}{(2M-3)(2M-1)^{1/2}}$ | $\frac{1}{2(M-1)}$ | $\frac{1}{2(M-1)}$ |

Note: FCW= first Chebyshev wavelet, SCW= second Chebyshev wavelet

## REFERENCES


1. Kaveh A, Hoseini Vaez SR, Hosseini P. Enhanced vibrating particles system algorithm for damage identification of truss structures, *Sci Iran* 2019; **26**(1): 246-56.
2. Kaveh A, Dadras A. Structural damage identification using an enhanced thermal exchange optimization algorithm, *Eng Optim* 2018; **50**(3): 430-51.
3. Kaveh A, Zolghadr A. Guided modal strain energy-based approach for structural damage identification using tug-of-war optimization algorithm, *J Comput Civil Eng* 2017; **31**(4): 04017016.

4. Kaveh A, Hoseini Vaez SR, Hosseini P, Fallah N. Detection of damage in truss structures using Simplified Dolphin Echolocation algorithm based on modal data, *Smart Struct Syst* 2016; **18**(5): 983-1004.
5. Kaveh A, Hosseini SM, Zaerreza A. Boundary strategy for optimization-based structural damage detection problem using metaheuristic algorithms, *Period Polytech Civil Eng* 2021; **65**(1): 150-67.
6. Kaveh A, Mahdavi VR. Damage identification of truss structures using CBO and ECBO algorithms. *Asian J Civil Eng* 2016; **17**(1): 75-89.
7. Koh P, Ghee C, Perry MJ. *Structural Identification and Damage Detection using Genetic Algorithms: Structures and Infrastructures*, CRC Press, 2009.
8. Kaveh A, Javadi SM, Maniat M. Damage assessment via modal data with a mixed particle swarm strategy, ray optimizer, and harmony search, *Asian J Civil Eng* 2014; **15**(1): 95-106.
9. Kaveh A, Maniat M. Damage detection in skeletal structures based on charged system search optimization using incomplete modal data, *Int J Civil Eng* 2014; **12**(2): 193-200.
10. Kaveh A, Zolghadr A. An improved CSS for damage detection of truss structures using changes in natural frequencies and mode shapes, *Adv Eng Softw* 2015; **80**: 93-100.
11. Kaveh A, Maniat M. Damage detection based on MCSS and PSO using modal data, *Smart Struct Syst* 2015; **15**(5): 1253-70.
12. Kaveh A, Zolghadr A. Cyclical parthenogenesis algorithm for guided modal strain energy based structural damage detection, *Appl Soft Comput* 2017; **57**: 250-64.
13. Brown AS, Ankireddi S, Yang HT. Actuator and sensor placement for multi-objective control of structures, *J Struct Eng* 1999; **125**: 757-65.
14. DeLorenzo ML. Sensor and actuator selection for large space structure control, *J Guidance, Control, Dyn* 1990; **13**(2): 249-57.
15. Haftka RT, Adelman HM. Effect of sensor and actuator errors on static shape control for large space structures, *AIAA J* 1987; **25**(1): 134-8.
16. Liu W, Hou Z, Demetriou MA. A computational scheme for the optimal sensor/actuator placement of flexible structures using spatial H2 measures, *Mech Syst Signal Process* 2006; **20**(4): 881-95.
17. Nestorović T, Trajkov M. Optimal actuator and sensor placement based on balanced reduced models, *Mech Syst Signal Process* 2013; **36**(2): 271-89.
18. Onoda J, Hanawa Y. Actuator placement optimization by genetic and improved simulated annealing algorithms, *AIAA J* 1993; **31**(6): 1167-9.
19. Xu YL, Chen B. Integrated vibration control and health monitoring of building structures using semi-active friction dampers: Part I—methodology, *Eng Struct* 2008; **30**(7): 1789-801.
20. Roh HS, Park Y. Actuator and exciter placement for flexible structures, *J Guidance, Control, Dyn* 1997; **20**(5): 850-6.

21. Cha YJ, Raich A, Barroso L, Agrawal A. Optimal placement of active control devices and sensors in frame structures using multi- objective genetic algorithms, *Struct Control Health Monitor* 2013; **20**(1): 16-44.
22. Abdullah MM, Richardson A, Hanif J. Placement of sensors/actuators on civil structures using genetic algorithms, *Earthq Eng Struct Dynam* 2001; **30**(8): 1167-84.
23. Guo HY, Zhang L, Zhang LL, Zhou JX. Optimal placement of sensors for structural health monitoring using improved genetic algorithms, *Smart Mater Struct* 2004; **13**(3): 528.
24. Liu W, Gao WC, Sun Y, Xu MJ. Optimal sensor placement for spatial lattice structure based on genetic algorithms, *J Sound Vib* 2008; **317**(1-2): 175-89.
25. Papadimitriou C. Optimal sensor placement methodology for parametric identification of structural systems, *J Sound Vib* 2004; **278**(4-5): 923-47.
26. Castro-Triguero R, Murugan S, Gallego R, Friswell MI. Robustness of optimal sensor placement under parametric uncertainty, *Mech Syst Signal Process* 2013; **41**(1-2): 268-87.
27. Mahdavi SH, Razak HA. Optimal sensor placement for time-domain identification using a wavelet-based genetic algorithm, *Smart Mater Struct* 2016; **25**(6): 065006.
28. Chang M, Pakzad SN. Optimal sensor configuration for flexible structures with multi-dimensional mode shapes, *Smart Mater Struct* 2015; **24**(5): 055012.
29. Li DS, Li HN, Fritzen CP. Load dependent sensor placement method: theory and experimental validation, *Mech Syst Signal Process* 2012; **31**: 217-27.
30. Ostachowicz W, Soman R, Malinowski P. Optimization of sensor placement for structural health monitoring: A review, *Struct Health Monitor* 2019; **18**(3): 963-88.
31. Wu ZY, Zhou K, Shenton HW, Chajes MJ. Development of sensor placement optimization tool and application to large-span cable-stayed bridge, *J Civil Structural Health Monitor* 2019; **9**(1): 77-90.
32. Beygzadeh S, Salajegheh E, Torkzadeh P, Salajegheh J, Naseralavi SS. Optimal sensor placement for damage detection based on a new geometrical viewpoint, *Int J Optim Civil Eng* 2013; **3**(1): 1-21.
33. Li B, Zhao YP, Wu H, Tan HJ. Optimal sensor placement using data-driven sparse learning method with application to pattern classification of hypersonic inlet, *Mech Syst Signal Process* 2021; **147**: 107110.
34. Yang C. Sensor placement for structural health monitoring using hybrid optimization algorithm based on sensor distribution index and FE grids, *Struct Control Health Monitor* 2018; **25**(6): e2160.
35. Lin JF, Xu YL, Law SS. Structural damage detection-oriented multi-type sensor placement with multi-objective optimization, *J Sound Vib* 2018; **422**: 568-89.
36. Mahdavi SH, Razak HA. A wavelet-based approach for vibration analysis of framed structures, *Appl Mathemat Computat* 2013; **220**: 414-28.
37. Mahdavi SH, Razak HA. Indirect time integration scheme for dynamic analysis of space structures using wavelet functions, *J Eng Mech* 2015; **141**(7): 04015006.

38. Mahdavi SH, Rofooei FR, Sadollah A, Xu C. A wavelet-based scheme for impact identification of framed structures using combined genetic and water cycle algorithms, *J Sound Vib* 2019; **443**: 25-46.
39. Zhu L, Wang Y. Second Chebyshev wavelet operational matrix of integration and its application in the calculus of variations, *Int J Comput Mathemat* 2013; **90**(11): 2338-52.